Ultrasound in Med. & Biol. Vol. 13, No. 9, pp. 555–566, 1987
Printed in the U.S.A.

0301-5629/87 $3.00 + .00

●*Original Contribution*

A PARTICULATE CONTRAST AGENT WITH POTENTIAL FOR ULTRASOUND IMAGING OF LIVER

K. J. PARKER and T. A. TUTHILL
The University of Rochester, Department of Electrical Engineering, Rochester, NY 14627, USA

and

R. M. LERNER and M. R. VIOLANTE
The University of Rochester, Department of Radiology, Rochester, NY 14627, USA

(*Received* 21 *October* 1986; *in final form* 20 *March* 1987)

Abstract—Ultrasonic backscatter and attenuation coefficients of a medium can be increased by the addition of solid, micron sized inhomogeneities. A potentially useful agent for ultrasonic contrast of liver images has been identified. Iodipamide ethyl ester (IDE) particles can be produced in the form of dense, relatively incompressible solids with high impedance mismatch to water. The chemical, biomechanical, and pharmacological properties of the small, uniform diameter IDE particles permit safe intravenous injection followed by rapid accumulation by reticuloendothelial (RE) cells of the liver and spleen, and later elimination from these organs. Since the particles are phagocytized by RE cells, present in normal liver but not in tumors and many lesions, the selective enhancement of ultrasonic backscatter should improve detectability of lesions which are hypo- or iso-echoic compared to surrounding tissue.

The mechanisms of particle-ultrasound interaction may be described by relative motion attenuation, and scattering from a cloud of dense, incompressible spheres for the case of IDE particles in agar. Thus, values of attenuation and backscatter can be controlled by choice of ultrasound frequency and particle concentration and size. When the particles are accumulated in rat livers, additional mechanisms induce attenuation and backscatter in excess of that predicted by IDE in agar. This preliminary work demonstrates that solid, biocompatible particles may be useful as an ultrasonic contrast agent.

Key Words: **Ultrasound, Contrast, Particles, Attenuation, Backscatter.**

INTRODUCTION

Conventional ultrasonic imaging is widely accepted for its ability to identify and, to a lesser extent, characterize focal liver disease. Cysts, abscesses, and tumors, both benign and malignant, may be characterized ultrasonographically by their reflectivity, attenuation, and gross morphology. The inherent contrast for fluid-containing lesions in the liver is relatively high permitting accurate detection, however, neoplastic liver lesions have variable ultrasonographic features which can be quite subtle.

Although the major imaging methods of radionuclide, CT, and ultrasound have relatively high sensitivities and specificities (ranging from 70%–90%), local variation may occur because of differences in interest and experience (Lind and Singer, 1986). CT and radionuclide imaging in some studies appear to have higher sensitivity than ultrasound for detecting hepatic metastases. Despite a suggested (10%–20%) lower sensitivity, ultrasound is frequently preferred for liver evaluation in both staging and follow up of therapy because of its availability, low cost, and easy patient acceptance (Anderson *et al.*, 1983).

Development of new contrast agents should enhance the ability to ultrasonically detect and measure hypo- and iso-echoic liver metastases accurately. Even a 10%–15% sensitivity gain would enhance the utility of ultrasound for primary screening, staging of malignant disease prior to treatment, and follow-up of already demonstrated liver metastases.

Much of the published literature on ultrasound contrast agents pertains to contrast echocardiology (Meltzer and Roeland, 1982). Since the first publications by Gramiak *et al.* (1969; Gramiak and Shah, 1968; Kremkau, Gramiak and Carstensen, 1968) the focus of this research has been contrast enhancement via microbubbles which generally range in size from

20 to 80 microns in diameter. While useful for echocardiography, unencapsulated microbubbles are not practical for intravenous administration with subsequent accumulation by, and enhancement of, the liver and spleen because the bubbles are cleared on first passage through the lungs. Hepatic and splenic contrast enhancement research has therefore utilized alternative approaches.

One approach to induce ultrasound contrast enhancement involved the intravenous administration in mice of aqueous solutions possessing a high speed of sound (Tyler, Ophir and Maklad, 1981). These same investigators evaluated the ability of collagen microspheres to enhance ultrasound backscatter in dog liver (Ophir *et al.*, 1980). Mattrey *et al.* (1982, 1983) have investigated the utilization of perfluorocarbon emulsions and Fink *et al.* (1985) studied lipid emulsions as potential contrast agents for hepatic sonography.

Despite these previous attempts to produce a contrast agent for hepatic ultrasonography, a clinically useful agent still is not available. New results using dense particles show possibilities for enhancing the contrast differential between liver parenchyma and metastases. Particulate contrast agents are accumulated in the liver only by Kupffer cells (Lauteala, Kormano, and Violante, 1984). Since liver lesions generally do not contain fixed phagocytic cells (McCredy, 1972), particulate agents selectively enhance only the normal functioning liver parenchyma and not the lesions. Metastases which are nearly isoechoic relative to liver parenchyma should be more easily detected following intravenous administration of a safe effective particulate contrast agent.

Iodipamide ethyl ester (IDE), a particulate iodinated contrast agent, has been evaluated for liver/spleen x-ray computed tomography image enhancement. Preliminary data indicates this particulate suspension might be useful for hepatic ultrasound image enhancement as well.

MATERIALS AND METHODS

Particle preparation and properties

Physical methods such as ball milling, grinding, or sonication for modifying and controlling particle size result in preparations with a very broad range of particle diameters. Both the biodistribution and the rate of solubilization of particulate materials vary with the size of the individual particles. To control these parameters a procedure for producing particles of a given size by chemical precipitation was developed. By adding an aqueous solution of polyvinylpyrrolidone, at controlled rates and temperatures, to

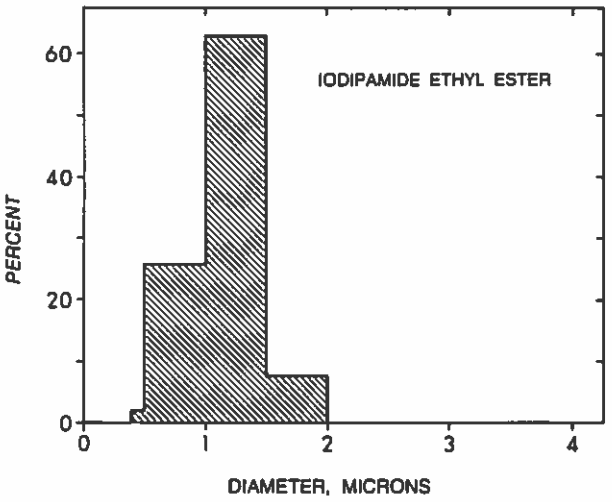

Fig. 1. The frequency distribution of particle diameters; mean diameter is 1.0 micron.

IDE dissolved in dimethylsulfoxide/ethanol, spherical particles are produced with an extremely narrow size distribution. This is demonstrated in Fig. 1 for particles with a mean diameter of 1.0 micron. The total range of particle diameters in this case is 0.4 to 2.0 microns with 90% of the particles ranging in size between 0.5 and 1.5 microns.

By carefully controlling precipitation parameters, particle preparations demonstrating different mean diameters, but with a similarly small range of diameters, can be produced.

The IDE particles produced using this methodology are stable in whole blood with no apparent tendency toward aggregation. Figure 2 shows that when suspended in whole blood, there is no tendency for the one micron IDE particles to aggregate with themselves or with the red blood cells. This figure also clearly shows the smooth contours of the IDE particles, as well as their size relative to human red blood cells.

The toxicity of IDE particles in mice is not as high as the parent compound iodipamide meglumine. Since only relatively low doses are necessary for image enhancements, IDE may have a higher safety index than currently used x-ray ionic and cholangiographic contrast agents (Violante and Fischer, 1986).

The fate of particles injected intravenously in saline suspension has been determined in previous rat experiments (Violante, Mare and Fischer, 1981). Within two hours, particles are almost exclusively accumulated by the RE cells of the liver, with approximately 5% in the spleen, and no detectable amounts in the bone marrow and lung or any other organ. This

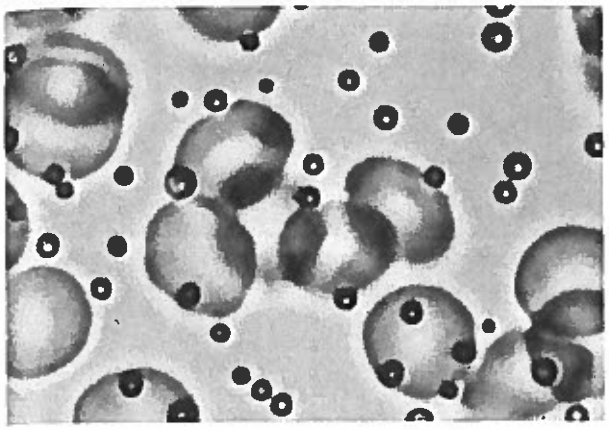

Fig. 2. A mixture of fresh iodipamide ethyl ester particles and human blood diluted with normal saline. Particle size is 0.5–1.5 micron diameter in comparison with red blood cells of 6–9 micron diameter. The mixture is very stable with no tendency toward aggregation. Magnification: 3350×.

liver-selective agent is phagocytized, dissolved, and eliminated from the organism within two days (Violante, Fischer and Mahoney, 1980; Violante, Mare and Fischer, 1981).

Sample preparation

For *in vitro* studies, saline suspensions of IDE particles were mixed into 2% agar during cooling. The mixtures were subjected to a vacuum while still fluid to remove entrapped air. No settling of particles was noted within agar samples because of the small particle sizes and increasingly high viscosity of agar as it cools. For *in vivo* experiments, sterile saline suspensions of IDE at 100 mg/cc were injected into the rat tail vein at a rate of 1 cc/min for a total dose of 157 mg/kg which produces liver concentrations of approximately 1.6 mg/g liver. Whole livers were excised from Wistar rats (125–175 g body weight) at 2 hours post injection, following euthanasia. The livers were placed immediately in chilled degassed saline, and massaged to eliminate any air bubbles. Samples of agar or liver were cut or packed under water to 1–2 cm thickness then placed in adjustable pill box shaped sample holders which employ thin plastic wrap covers. The plastic film in tension creates smooth, parallel surfaces which are ideal for laboratory ultrasound measurements. The effects of the plastic film are small and can be eliminated from measurements. All measurements were taken at 21°–22°C.

Attenuation measurements

Amplitude attenuation coefficients were obtained via radiation force-insertion loss technique; which has the advantage of being a phase insensitive measurement. An anechoic chamber was developed with a linear array of 1 inch diameter ceramic piezoelectric transducers with resonant frequencies near 0.5, 1, 2, 3, 4, and 5 MHz. Each transducer generates a collimated beam (for at least 7 cm) with total acoustic power variable from 10 mW to 10W. Each transducer is capable of efficient output at its fundamental and odd harmonics, enabling the generation of precisely calibrated beams at over 15 discrete frequencies between 0.5 and 15 MHz. For attenuation measurements, an absorbing rubber float intercepts the collimated ultrasonic beam, and the radiation force before and after insertion of a sample is precisely measured using a Sartorius microbalance with resolution of 5 mW of acoustic output. Accuracies of ±5% are possible in homogeneous materials (Parker and Lyons, in press).

Backscatter experiments

Backscatter data were obtained semi-quantitatively by scanning specimens with commercial B-scan imaging devices. We utilized a variety of real time instruments employing mechanical and electronic sector scanning, with a range of frequencies from 3.5 to 10 MHz. Scanning of samples was performed using real time sector scanners using flat TGC and standard (1 dB/cm/MHz for liver, 0.3 dB/cm/MHz for agar) settings at each of 3.5, 5, 7, and 10 MHz. By employing reference materials including agar, normal livers, phantoms, and graded concentrations of particles, it was possible to estimate relative changes in backscatter, in dB, from the grey scale speckle pattern of the B-scan image.

RESULTS

Attenuation

Suspensions of 1.0 μm IDE particles in agar produced a linear increase in attenuation with increasing particle concentration. Figure 3 shows attenuation divided by frequency, α/f, values obtained at 5 MHz for 2% agar with 0%, 1.8%, and 5.2% by weight IDE particles. These data demonstrate an excess attenuation of approximately 8.3×10^{-3} np/cm per mg, at 5 MHz.

Attenuation also increased with particle size, though not linearly, as shown in Fig. 4. Attenuation divided by frequency measured at 5 MHz is shown for 3.2 mg/ml agar concentration of IDE particles with mean diameters of 0.1, 0.5, and 1.0 μm.

The frequency dependence of attenuation was also found to be dependent on particle size. Figure 5 shows attenuation divided by frequency as a function of frequency for plain 2% agar, and agar suspensions

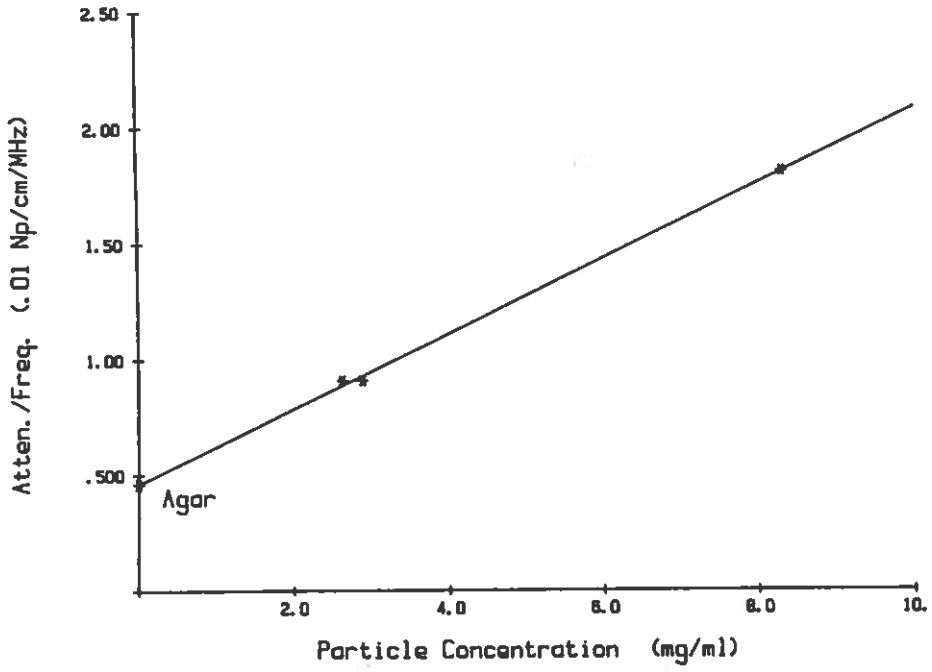

Fig. 3. Attenuation (divided by frequency in np/cm-MHz) at 5 MHz versus concentration of 1 μm IDE particles in agar. Starting from the value of plain 2% agar at approximately 5×10^{-3} np/cm-MHz; the excess attenuation increases linearly with concentration, as expected for dilute suspensions.

of 0.2, 0.6, and 1.0 μm IDE particles at 3.2 mg/ml. The smooth curves are least square error fits to a power law $\alpha(f) = \alpha_0 f^n$. The 0.2 μm particle suspension has the highest frequency dependence of $n = 1.39$, compared to $n = 1.20$ for the 0.5 μm and $n = 1.16$ for the 1.0 μm particles.

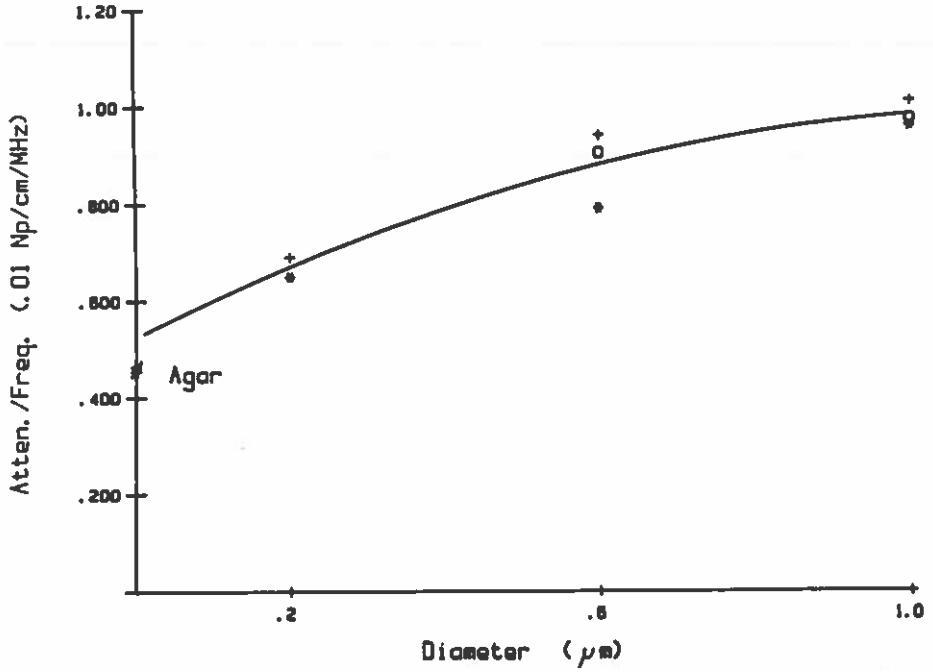

Fig. 4. Attenuation (divided by frequency) at 5 MHz for plain 2% agar and suspensions of 3.2 mg/ml IDE particles with diameters of 0.2, 0.6, and 1.0 μm. The trend is towards increasing attenuation with increasing diameter, although the relationship is not linear.

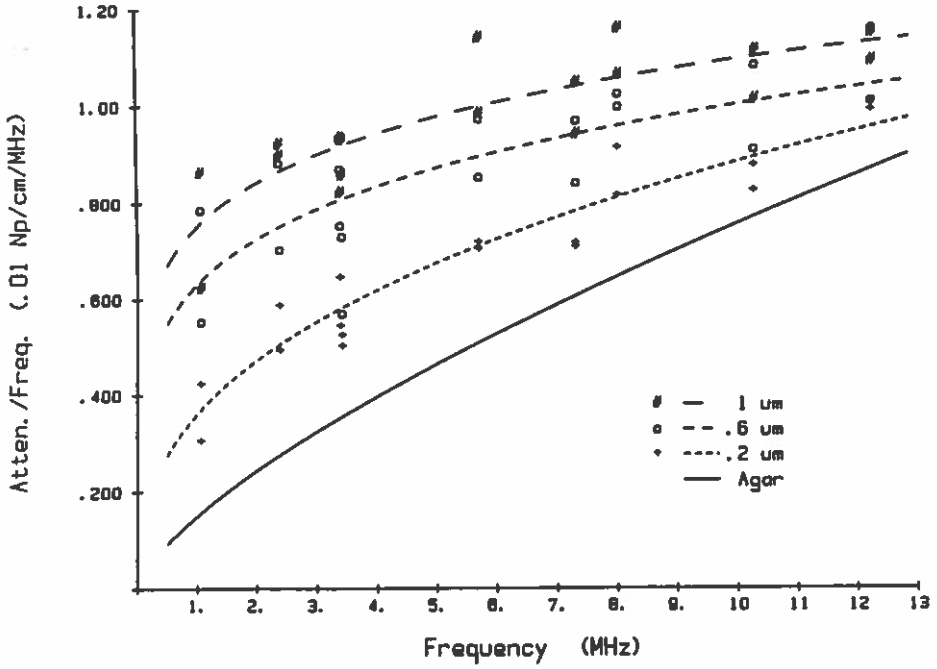

Fig. 5. Attenuation (divided by frequency) versus frequency for various diameters of IDE particles at 3.2 mg/ml concentration in 2% agar. Symbols are: (#) 1.0 μm; (O) 0.6 μm; (+) 0.2 μm; and smooth lines are power law fits to the data. The trend is towards higher attenuation with increasing diameter, but the frequency dependence of attenuation also changes with particle size.

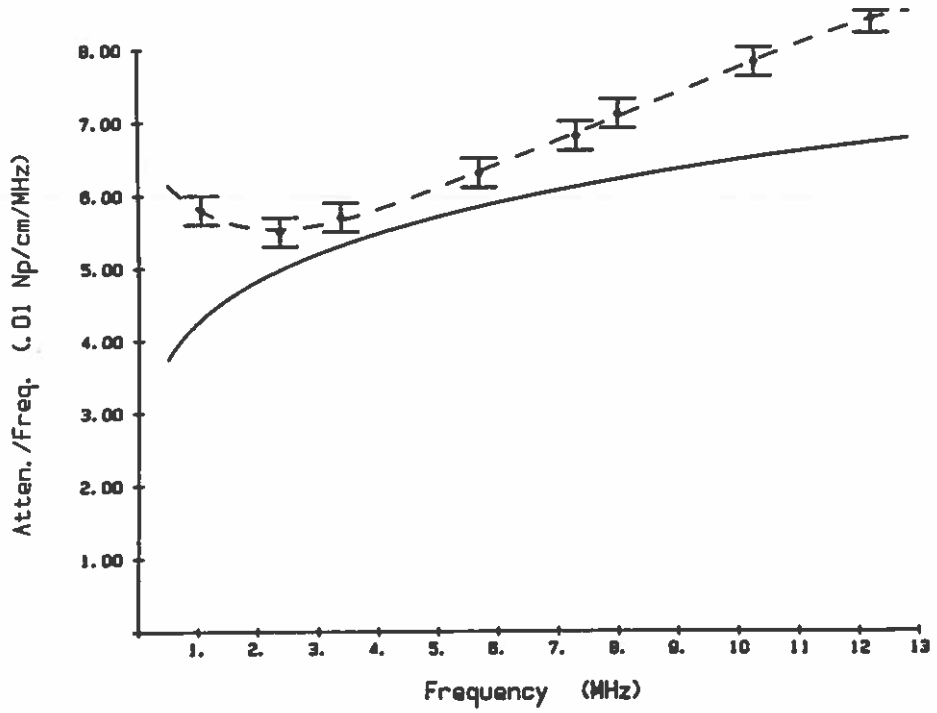

Fig. 6. Attenuation (divided by frequency) versus frequency for normal rat livers and rat livers with approximately 1.6 mg/cc of 1.0 μm IDE particles, excised 2 hours following intravenous injection of particulate suspension. Solid line (lower) is a power law curve fit to mean values of 25 normal livers (sd ± 7% not shown). Data points (upper) are mean and single sd for a group of 4 livers with IDE particles. The excess attenuation resulting from particle uptake in liver is different from that found in agar, possibly indicating additional interactions such as the aggregation of particles by Kupffer cells.

In rat livers, attenuation divided by frequency was also increased by the presence of IDE particles. Figure 6 shows values for normal rat livers and those with approximately 1.0 mg/cc of 1.0 μm IDE particles, excised 2 hours following intravenous injection of particulate suspension. In the case of liver, increased attenuation caused by particle addition is higher than would be expected from agar studies. Furthermore, the frequency dependence of attenuation is unlike agar IDE, indicating additional tissue-particle-ultrasound interactions.

Backscatter

The effect of particle concentration was evaluated from the overall speckle brightness in 10 MHz B-scan images of agar suspensions of 1.0 μm particles at 8 mg/cc and 3.2 mg/cc. Figure 7 shows the result, with detectable brightness increase in the top, higher concentration block. Flat TGC curves were used in these scans, but the contrast differences were evident under ramped TGC curves as well. Contrast was also evident at 7 and 5 MHz on other B-scan instruments.

To quantify the backscatter coefficient, comparisons were made against 30% suspension in saline of washed, heparinized, unclotted, dog red blood cells, which have a reported backscatter coefficient on the order of 10^{-5} $(cm\text{-}sr)^{-1}$, depending on hematocrit and flow conditions (Fei and Shung, 1985; Shung *et al.*, 1984). Figure 8 shows comparisons of 8 and 3.2 mg/cc suspensions of particles in agar imaged under identical conditions as a plastic container filled with a 30% solution of RBCs in saline. A thin plastic membrane covers the red blood cell suspension preventing mixing with coupling water. At 10 and 7 MHz, the IDE suspensions appeared brighter with larger saturated regions of speckle. This would indicate roughly 5–15 dB relative increase in the backscatter coefficient of IDE suspensions over 30% red blood cells in saline.

Liver contrast was evident at 10 and 7 MHz B-scan images. Figures 9a and b show different cross-sections of excised rat livers packed in a sample holder, with the top layer containing 3.2 mg/cc of 1.0 μm IDE particles, and the bottom layer normal livers. The treated livers appear hyperechoic compared to the controls.

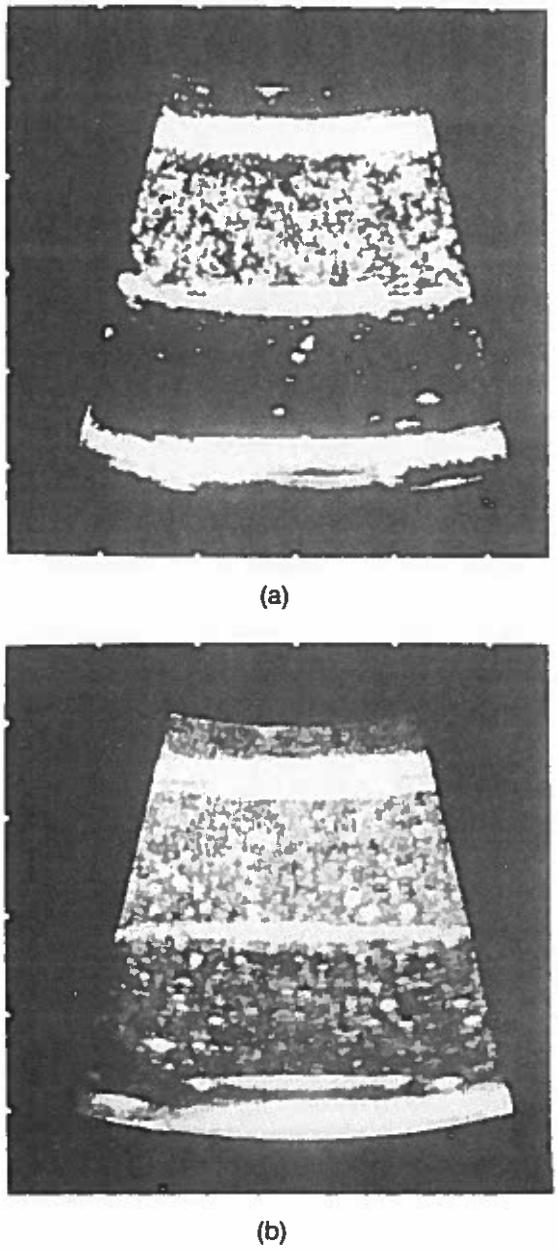

Fig. 7. B-scan images of agar blocks using a 10 MHz sector scanner. In (a) the top medium with bright speckle is 8 mg/cc of 1.0 μm IDE particles in 2% agar. The bottom material, with few echoes, is plain 2% agar. In (b), the top agar block contains 8 mg/cc and the bottom block 3.2 mg/cc of 1.0 μm IDE particles. These demonstrate the increase in backscatter (thus image brightness) with concentration of particles.

DISCUSSION

Attenuation

In soft tissues (*i.e.* liver) or media (*i.e.* agar-gelatin) comprised mostly of water with small amounts of proteins, fat, and other compounds, the ultrasonic attenuation has been shown to be determined largely by absorption mechanisms, with scattering mechanisms contributing only a fraction of the overall losses (Parker, 1983; Campbell and Waag, 1984; Lyons and Parker, in press). Absorption is caused by multiple relaxation mechanisms at the macromolecular level (Kremkau and Carstensen, 1972; Kremkau and Cowgill, 1984).

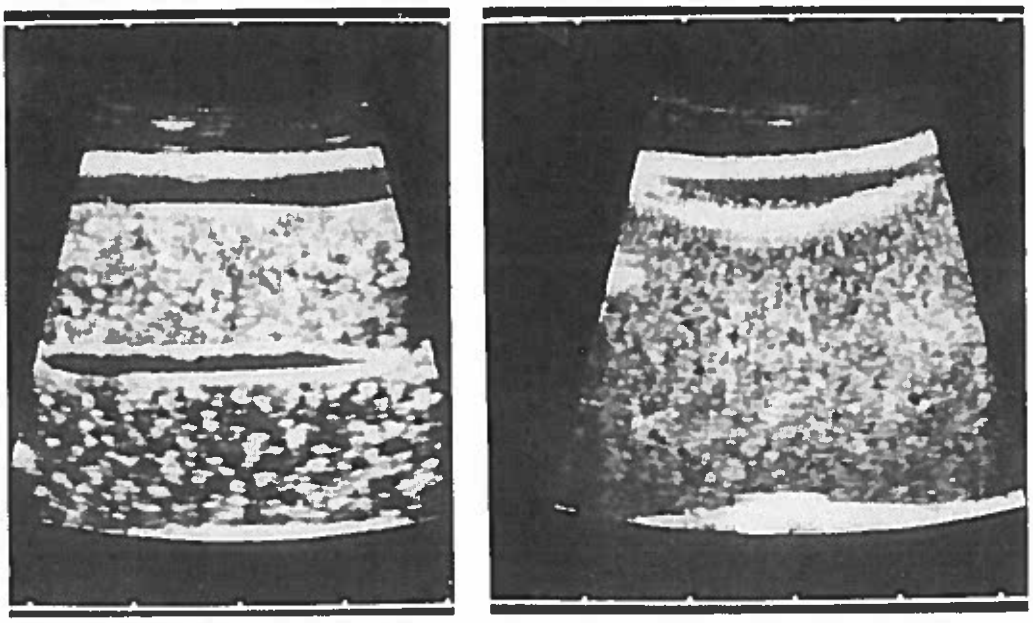

(a) (b)

Fig. 8. 10 MHz B-scan images of 8 and 3.2 mg/cc, 1 μm IDE particles in 2% agar (a), and 30% red blood cells suspended in saline (b). The images were taken sequentially in the same water tank under identical TGC and instrument settings. Using literature values of the backscatter coefficient of the red blood cell suspension, we can conclude that at 10 MHz, the IDE suspensions in agar have a backscatter coefficient on the order of 10^{-5} $(\text{cm-sr})^{-1}$. This agrees with calculations based on the long wavelength approximation for scattering from dense, incompressible spheres.

The addition of IDE particles increases attenuation of experimental samples. The presence of a dense particle in a soft medium creates scattering and local losses (heating) due to the acoustic impedance mismatch. A body of theory has been developed to treat the presence of such particles (Fry, 1952; Carstensen and Schwan, 1959a, 1959b; Allegra and Hawley, 1972). The absorption mechanism has been called *relative motion*, since under plane wave excitation, a difference exists between the sinusoidal displacements of the dense particle and the medium (at uninfluenced positions a few diameters from the particle). This relative motion, coupled with viscosity of the medium, generates a frictional loss per particle, per acoustic cycle which directly contributes to an overall material attenuation coefficient.

The relative motion attenuation coefficient can be shown to increase linearly with particle concentration, and as the square of density difference between the particles and the surrounding medium. The dependence on diameter, and medium viscosity are complicated functions of frequency, but in general, at any fixed frequency, the attenuation increases with increasing particle size and fluid viscosity. Figure 10 depicts the theoretical frequency dependence of attenuation (divided by frequency) for different diameter particles at 3.2 mg/cc suspended in water (negligible attenuation) with fluid viscosity of 0.01 poise. The peak value of attenuation/frequency is seen to shift to the right (to higher frequencies) as particle size decreases.

The theory of relative motion provided a good match to measured values of particles in agar. Using particle values of: diameter = 1.0 μm; concentration = 3.2 mg/cc, and density = 2.4 g/cm^3; with agar viscosity = 0.01 poise, values of attenuation over a frequency range of 0.5 to 13 MHz were calculated and added to measured baseline attenuation values of 2% agar. (Superposition or addition of attenuation mechanisms is permissible as long as the attenuation per wavelength is much less than unity, a condition satisfied in all situations presented herein.) The resulting combined attenuation is shown in Fig. 11 as a solid line. The measured data for 1.0 μm particles at approximately 3.2 mg/cc closely matched attenuation calculations based on the theory of relative motion and known baseline values of agar attenuation. Other comparisons demonstrated that the theory provided a good match to measured attenuation values of particles of different diameters (0.6 μm, 0.2 μm) and different concentrations (0.8–8.8 mg/cc). Thus, the ultrasonic attenuation of these high density particles as randomly positioned inhomogeneities within a viscous medium appears to be well described by the

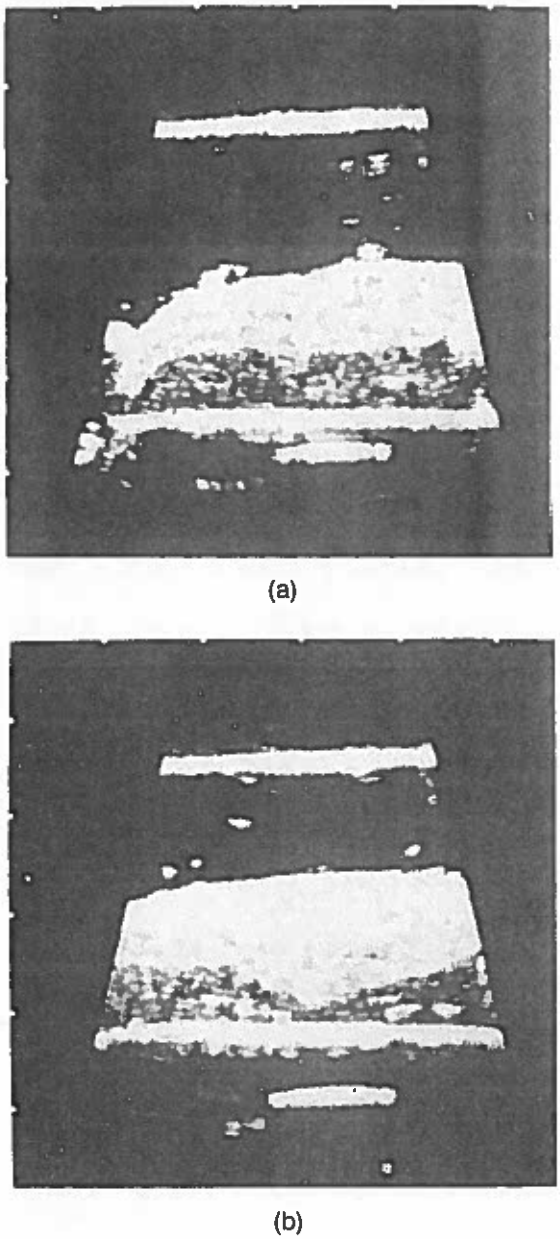

Fig. 9. 10 MHz B-scan images of excised rat livers following intravenous injection of IDE particles or saline. Four livers are packed between thin plastic films with the top, hyperechoic layer comprised of two side-by-side livers with 3.2 mg/cc of 1 μm IDE particles. The botton, hypoechoic layer is composed of normal liver lobes. Different cross sections are shown in (a) and (b). These demonstrate that particle uptake by normal liver parenchyma results in hyperechoic speckle.

theory of relative motion. This theory by itself is insufficient to explain the excess attenuation measured in rat liver (Fig. 6), because of the higher loss in liver, especially at low (1–2 MHz) and high (10–12 MHz) frequencies. An additional factor in liver is the active agglomeration of particles by Kupffer cells, which accumulate an average of 6–12 particles per cell, with some cells containing as many as 30 particles (Lauteala, Kormano and Violante, 1984). The ultrasonic beam may interact with an intracellular agglomeration as a larger effective diameter particle. There is also a possibility of multiple scattering effects because of the strong impedance mismatch and close packing of individual particles within the RE cells.

Backscatter

The relevant theory for scattering from solid, small (0.1–10 μm particles) IDE particles with incident ultrasound in the 1–10 MHz band (1.5–0.15 mm wavelengths) may be characterized by the long wavelength approximations for a cloud of dense, incompressible spheres. Under these conditions the backscattered energy can be shown to be proportional to the sixth power of sphere radius, the fourth power of frequency, the square of density difference between particles and medium, and the first power of particle concentration (Morse and Ingard, 1968). In this regime, scattering patterns have a directivity peak towards the backscatter (180°). In agar and rat liver experiments presented in previous sections, typical parameter values include a density difference of 2.4 g/cc for particles versus 1.0 g/cc for H_2O, and IDE concentrations of 10^9 to 10^{10} particles/cc. Calculations using the long wavelength approximation indicate backscatter coefficient increases on the order of 10^{-6} to 10^{-5} $(cm\text{-}sr)^{-1}$ (at 10 MHz) when these doses of IDE particles are distributed throughout liver or agar. Images of IDE/agar and 30% suspension of RBCs in saline independently support the case for backscatter coefficient on the order of 10^{-5} $(cm\text{-}sr)^{-1}$ at 10 MHz. However, normal rat liver presumably has a backscatter coefficient much greater than that of blood, thus an increase in backscatter on the order of 10^{-5} $(cm\text{-}sr)^{-1}$ would not necessarily enhance brightness. Nonetheless, images of rat livers with and without particles show unequivocal increase in backscatter with IDE. Thus the IDE contrast enhancement in liver appears to be greater than that occurring in agar/particle suspensions. Again, the agglomeration of particles by Kupffer cells may influence the backscatter coefficient *in vivo*.

The same scattering model shows that contribution of total scattered power to attenuation is approximately 3 orders of magnitude below the relative motion contribution, at 10 MHz. Thus, scattering from these inhomogeneities does not significantly influence the absorption coefficient.

To be effective as a clinical ultrasound contrast agent, the solid particles will require sufficient back-

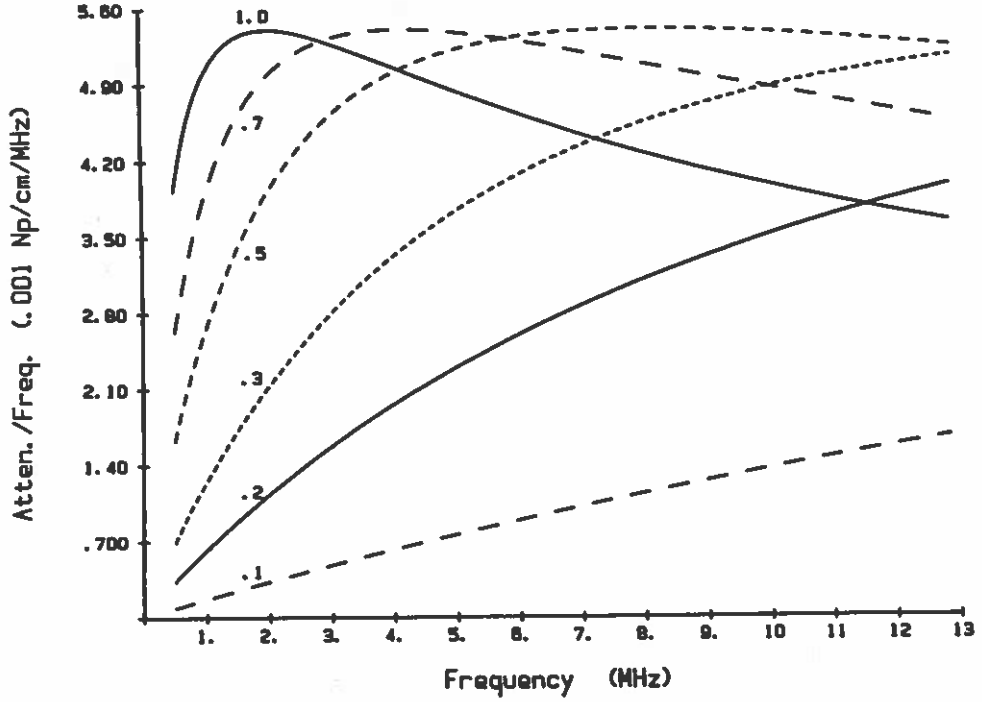

Fig. 10. Theoretical plots of attenuation (divided by frequency) versus frequency, for 3.2 mg/cc concentrations of IDE particles, using the theory of relative motion. Numbers shown are particle diameters in microns, ranging from 0.1 to 1.0. The frequency dependence of attenuation is shown to be a strong function of particle diameter.

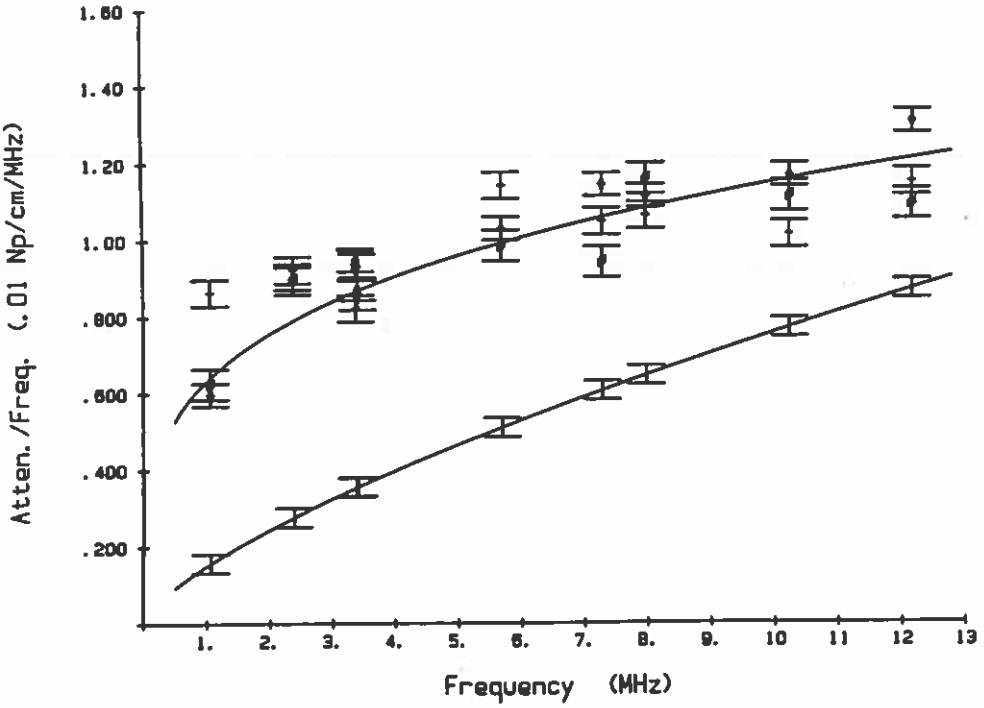

Fig. 11. Attenuation (divided by frequency) versus frequency for plain 2% agar (lower), and agar with 3.2 mg/cc of 1.0 μm IDE particles (mean and 1 sd shown for 3 different samples of 3.2 mg/cc particle suspensions). The solid line for agar represents a curve fit, whereas the solid line for agar-IDE suspension (top) is a theoretical curve obtained using relative motion to predict the excess attenuation caused by 1.0 μm particles. This theory provides a good description of the magnitude and frequency dependence of attenuation of IDE suspensions in agar.

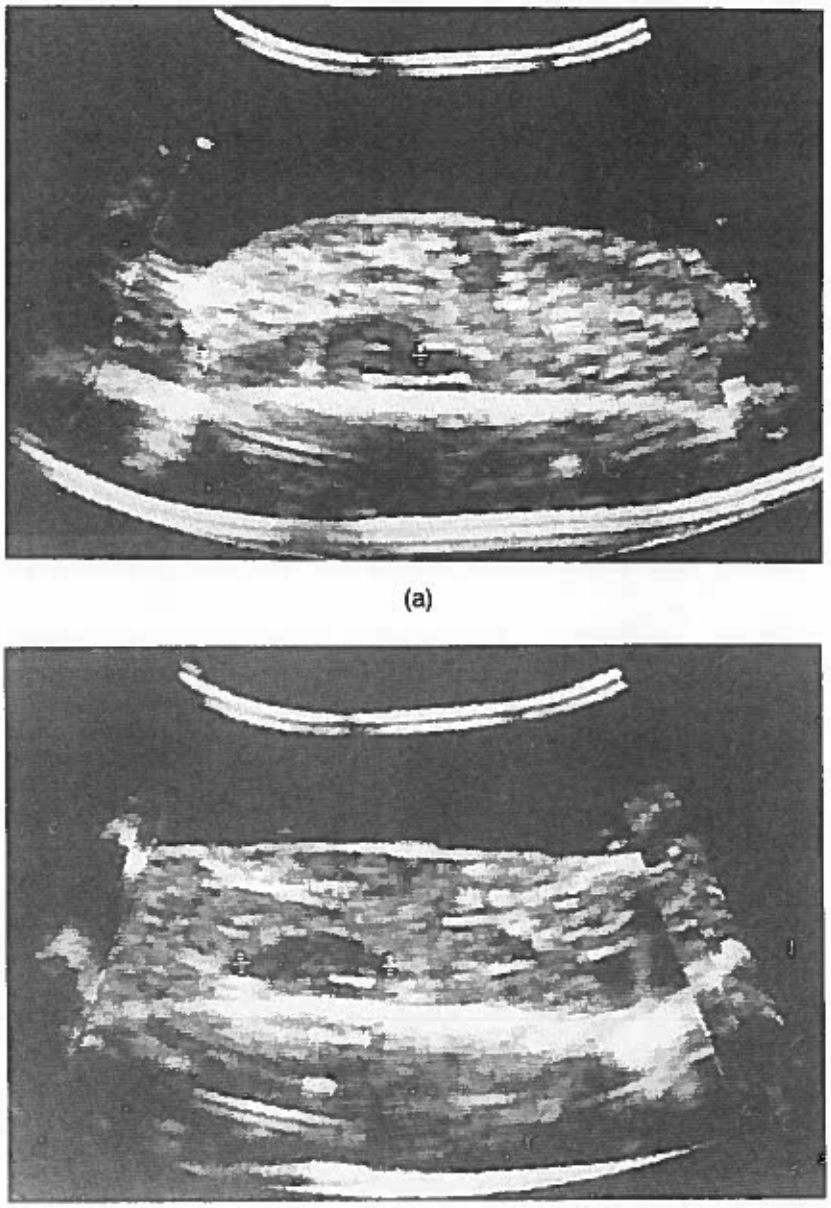

Fig. 12. B-scan images from a 7 MHz sector scanner, of IDE livers surrounding a single normal liver. The lobes are packed between thin plastic films, with the normal liver in the lower left quadrant, indicated by cursors. The normal liver appears hypoechoic compared to the livers with 3.2 mg/cc of 1.0 μm particles. Parts (a) and (b) are different cross-sections of the packed liver layers. These images represent contrast enhancement of an initially isoechoic tumor region in liver. After particle uptake by surrounding normal parenchyma, the "tumor" is clearly defined as a hypoechoic region.

scatter enhancement against normal human liver parenchyma, at lower frequencies (3–5 MHz) commonly used in abdominal images. We recognize that the particle backscatter coefficient falls with decreasing frequency, and our examples utilized 10 MHz images. Nonetheless, some considerations indicate the applicability to lower frequency abdominal imaging. Figure 12 shows 7 MHz cross-section images of packed, excised IDE livers surrounding a single normal liver lobe. The normal lobe appears hypoechoic, as would a tumor or lesion in liver which, lacking normal RE cells, would not accumulate solid particles. Despite the lower frequency (and resolution) compared to the earlier images of Figs. 7 and 8, the contrast is still evident. The lack of resolution at lower frequencies (3.5–5 MHz) made it impossible to

interpret images of the small rat livers. Since the initial results at higher frequencies are encouraging, further studies using larger animals (dogs) and lower frequencies seem justified.

Another area of research concerns the optimization of the mechanical and chemical properties of the compound, so that higher backscatter coefficients are obtained *in vivo* with the highest possible margin of safety. Since backscatter increases as the square of density difference, compounds with density greater than IDE, produced as a particulate suspension, may be better contrast agents. Similarly, increased particle compressibility could be achieved by increasing the lipid component of the molecules, while more ionic compounds (which pack tightly in crystalline latices) should have decreased compressibility relative to IDE. Thus while IDE particles are a promising start for x-ray and ultrasound contrast enhancement, it is possible that a related compound with optimized ultrasonic and safety properties can be produced.

The optimum particle size has not yet been determined for use in livers. In agar, attenuation and scattering increase with size, the latter coefficient depending on the sixth power of diameter. However, safety considerations limit particle sizes to less than 5 μm *in vivo*, since potential blocking of capillaries and small venules and arterioles is possible with larger particles. Also, initial rat liver studies indicate that the accumulation of smaller particles into a larger effective sphere by RE cells may play an important role in the backscatter enhancement. Thus, it is possible that smaller diameter particles (0.1–1.0 μm) which are easily aggregated by Kupffer cells may prove more effective than larger (3–5 μm) particles.

SUMMARY

Solid particles, which have higher density and lower compressibility than water, can be used for liver ultrasound contrast agents. The introduction of these inhomogeneities into a medium increases both the backscatter and attenuation coefficients; however the increase in attenuation is not so great as to mask the enhanced backscatter. The magnitude of excess attenuation and backscatter at any frequency can be controlled by varying particle size and concentration. Further optimization of particle mechanical and chemical properties may be possible so that the greatest possible contrast enhancement can occur at the lowest dose. In agar, the excess attenuation can be described by the theory of relative motion, and backscattering by the long wavelength approximations for a cloud of dense, incompressible spheres. In liver, however, the increased attenuation and backscatter exceed values expected from agar studies. This indicates additional tissue-particle interactions, of which accumulation of particles in groups of 5 or more by Kupffer cells may play an important role.

Acknowledgments—We are indebted to Ms. J. Ventura for her technical assistance. This work was supported by NSF Grant ECE-8643973, and the Whitaker Foundation.

REFERENCES

Allegra J. R. and Hawley S. A. (1972) Attenuation of sound in suspensions and emulsions: theory and experiments. *J. Acoust. Soc. Am.* **51**, 1545–1564.

Anderson P. *et al.* (1983) Computed tomography, ultrasound and scintigraphy of the liver in patients with colon or breast carcinoma, a prospective comparison. *Radiology* **149**, 225–230.

Campbell J. A. and Waag R. C. (1984) Measurements of calf liver ultrasonic differential and total scattering cross sections. *J. Acoust Soc. Am.* **75**, 603–611.

Carstensen E. L. and Schwan H. P. (1959a) Absorption of sound arising from the resence of intact cells in blood. *J. Acoust. Soc. Am.* **31**, 185–189.

Carstensen E. L. and Schwan H. P. (1959b) Acoustic properties of hemoglobin solutions. *J. Acoust. Soc. Am.* **31**, 305–311.

Fei D. Y. and Shung K. K. (1985) Ultrasonic backscatter from mammalian tissues. *J. Acoust. Soc. Am.* **78**(3), 871.

Fink I. J., Miller D. J., Shawker T. H. *et al.* (1985) Lipid emulsions as contrast agents for hepatic sonography: an experimental study in rabbits. *Ultras. Imaging* **7**, 191.

Fry W. F. (1952) Mechanism of acoustic absorption in tissue. *J. Acoust. Soc. Am.* **24**, 412–415.

Gramiak R. and Shah P. M. (1968) Echocardiography of the aortic root. *Invest. Radiol.* **3**, 356.

Gramiak R., Shah P. M. and Kramer D. H. (1969) Ultrasound cardiography: contrast studies in anatomy and function. *Radiology* **92**, 939.

Kremkau F. W., Gramiak R., Carstensen E. L. *et al.* (1968) Ultrasonic detection of cavitation at catheter tips. *Am. J. Roentgenol.* **3**, 159.

Kremkau F. W. and Carstensen E. L. (1972) Macromolecular interaction in sound absorption. *Proceedings of Workshop on Interaction of Ultrasound and Biological Tissues*, pp. 37–42. Battelle Seattle Research Center, Food and Drug Administration, U.S. Department of Health, Education and Welfare, Rockville, MD.

Kremkau F. W. and Cowgill R. W. (1984) Biomolecular absorption of ultrasound I molecular weight *J. Acoust. Soc. Am.* **76**(5), 1330–1335.

Lauteala L., Kormano M. and Violante M. R. (1984) Effect of intravenously administered iodipamide ethyl ester particles on rat liver morphology. *Invest. Radiol.* **19**, 133.

Lind S. E. and Singer D. E. (1986) Diagnosing liver metastases. *J. Clin. Oncol.* **4**, 379–388.

Lyons M. D. and Parker K. J. (in press) Attenuation and absorption in soft tissue II—experimental results. *IEEE UFFC.*

Mattrey R. F., Scheible F. W., Gosink B. B. *et al.* (1982) Perfluoroctylbromide: a liver/spleen-specific and tumor-imaging ultrasound contrast material. *Radiology* **145**, 759.

Mattrey R. F., Leopold G. R., Van Sonnenberg E. *et al.* (1983) Perfluorochemicals as liver- and spleen-seeking ultrasound contrast agents. *J. Ultras. Med.* **2**, 173.

McCredy R. (1972) Scintigraphic studies of space-occupying liver disease. *Seminars in nuclear medicine*, **2**, 108.

Meltzer R. S. and Rocland T. J. eds. (1982) Contrast echocardiography. In *Developments in Cardiovascular Medicine*, Vol. 15. Martinus Nijhoff Publishers, The Hague, Boston, London.

Morse P. M. and Ingard C. (1968) *Theoretical Acoustics* (Chap. 8, pp. 427–428). McGraw Hill, New York.

Ophir J., Gobuty A., McWhirt R. E. and Maklad N. F. (1980) Ultrasonic backscatter from contrast producing collagen microspheres. *Ultras. Imaging* **2**, 67.

Parker K. J. (1983) Ultrasonic attenuation and absorption in liver tissue. *Ultrasound in Med. & Biol.* **9**, 363–369.

Parker K. J. and Lyons M. E. (in press) Attenuation and absorption in soft tissue I—calibration and error analyses. *IEEE UFFC*.

Shung K. K. *et al.* (1984) Effect of flow disturbance on ultrasonic backscatter from blood. *J. Acoust. Soc. Am.* **75**(4), 1265.

Tyler T. D., Ophir J. and Maklad N. F. (1981) *In vivo* enhancement of ultrasonic image luminance by aqueous solutions with high speed of sound. *Ultras. Imaging* **3**, 323.

Vermess M., Doppman J. L., Sugarbaker P. *et al.* (1980) Clinical trials with a new intravenous liposoluble contrast material for computed tomography of the liver and spleen. *Radiology* **137**, 217.

Violante M. R., Fischer H. W. and Mahoney J. (1980) Particulate contrast media. *Invest. Radiol.* **15**, s329.

Violante M. R., Fisher H. W., Mare K. O. *et al.* (1981) Maximizing hepatic contrast enhancement with particulate contrast agents in computed tomography. *Contrast Media in Computed Tomography* (Edited by R. Felix, E. Kazner and O. H. Wegener), pp. 69–75. Excepta Medica, Amsterdam-Oxford-Princeton.

Violante M. R., Mare K. and Fischer H. W. (1981) Biodistribution of a particulate hepatolienographic CT contrast agent: a study of iodipamide ethyl ester in the rat. *Invest. Radiol.* **16**, 40.

Violante M. R. and Fisher H. W. (1986) *Contrast Media: Biological Effects and Clinical Application* (Chap. VII). CRC Press, Boca Raton, Florida.